J|A|C|S
COMMUNICATIONS

Published on Web 05/29/2008

Trapping and Structural Elucidation of a Very Advanced Intermediate in the Lesion-Extrusion Pathway of hOGG1

Seongmin Lee, Christopher T. Radom, and Gregory L. Verdine*

Department of Chemistry and Chemical Biology, Harvard University, Cambridge, Massachusetts 02138

Received February 1, 2008; E-mail: verdine@chemistry.harvard.edu

DNA glycosylases, key components of the base-excision DNA repair pathway,[1,2] recognize damaged nucleobases in DNA and catalyze their excision. Structural studies have revealed that structurally diverse DNA glycosylases share the common feature of extruding their target lesion from DNA and inserting it into an extrahelical active site pocket on the enzyme; only after this does catalysis ensue.[3] We have shown that this extrusion process proceeds via a multistep pathway characterized by discrete pre- and postextrusion intermediates.[4a] In a series of structural studies,[4] we have captured human 8-oxoguanine DNA glycosylase (hOGG1) bound to DNA at different stages along the extrusion pathway for its cognate lesion, the mutagen 8-oxoguanine (oxoG).[5] None of these studies, however, revealed a catalytically active hOGG1 presenting oxoG to the active site. Here we report the first synthesis of a photocaged analogue of oxoG, and the use of this derivative in combination with flash-cryotrapping to capture and structurally characterize the most advanced intermediate yet observed along any base-extrusion pathway. The structure reveals that insertion of the lesion nucleobase into the enzyme active site occurs much faster than subsequent rearrangements in active site side-chains that produce a catalytically active state.

In previous work,[4a] we used intermolecular disulfide cross-linking (DXL) technology[6] to capture hOGG1 attempting to present the normal base G to its active site pocket. The structure of this G-interrogation complex revealed that the target G, though fully extrahelical, failed to insert into the active site pocket, and instead resided in a nearby 'exosite'. We reasoned that an oxoG base affixed with a photocleavable group at the O^6-position might similarly be denied entry in the lesion-recognition pocket, owing to a steric clash between the bulky photocleavable group and active site residues (Figure 1). If so, then photodeprotection would liberate the oxoG and thereby trigger the final sequence of the base-extrusion pathway, namely transit of the oxoG from the exosite to the active site. We hoped that irradiation of the caged complex followed by flash-freezing might lead to the cryogenic trapping of an intermediate in either base-extrusion or in base-excision. To stabilize the otherwise unstable complex formed between hOGG1 and DNA containing the photocaged-oxoG DNA complex, we employed DXL technology, just as with the G-complex and other extrusion intermediates (Figure 1).[4]

The synthesis of O^6-photocaged oxoG DNA began with O-acetylation of 2′-deoxyguanosine **1** (Scheme 1). Protection of the N^2-amine followed by bromination provided 8-bromo-2′-deoxy guanosine **2**. Mitsonobu coupling gave the O^6-*o*-nitrophenisopropyl ether **3** (as a mixture of stereoisomers); this was converted to 8-oxo-2′-deoxyguanosine **4** by treatment with sodium acetate. Following removal of the 3′ and 5′-acetyl groups, the free nucleoside (not shown) was elaborated into the corresponding O^6-photocaged oxoG phosphoramidite **5**, which was then employed in the solid phase synthesis of **6**, a 16-mer oligodeoxynucleotide bearing a single O^6-photocaged 8-oxoG residue (5′-AGCGTCCA**X**GTCTACC-3′; **X** =

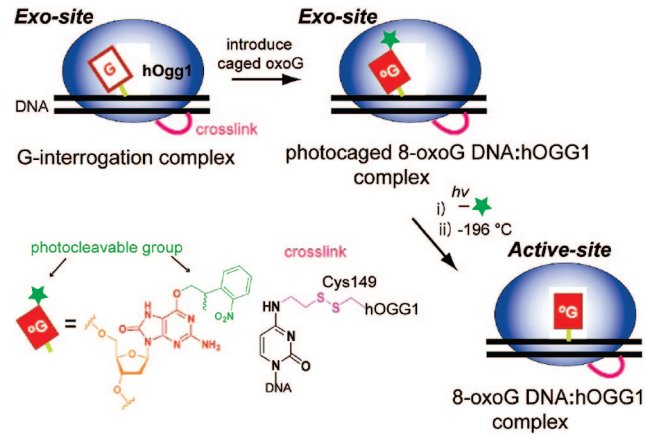

Figure 1. Overview of the experimental strategy

Scheme 1. Preparation of DNA Containing a Photocaged oxoG [a]

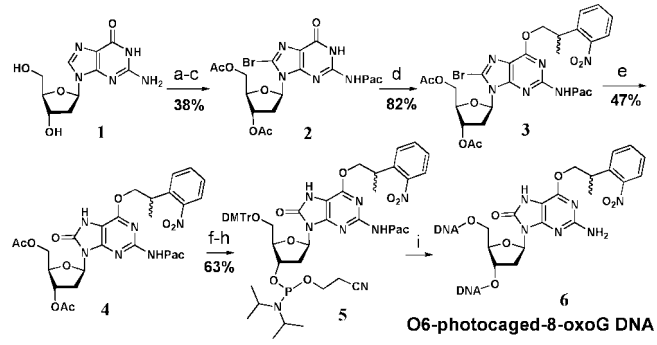

[a] Reagents and conditions: (a) Ac_2O, DMAP, MeCN, 25 °C, 3 h; (b) PacCl, pyridine, 0 °C; (c) NBS, pyridine (2 equiv), MeCN, 25 °C; (d) PPh_3, DEAD, 2-(2-nitrophenyl)propanol, THF, 25 °C; (e) NaOAc, AcOH, 80 °C; (f) 1 N NaOH, EtOH, 0 °C; (g) DMTrCl, pyridine, 25 °C; (h) 4,5-dicyanoimidazole, 2-cyanoethyltetraisopropyl phosphordiamidite, CH_2Cl_2, 25 °C; (i) solid phase DNA synthesis.

O^6-photocaged oxoG). The oligonucleotide was deprotected with methanolic potassium carbonate, purified by urea-PAGE gel electrophoresis, and its structure was verified by MALDI-TOF analysis. The photocaged nucleotide was annealed to a complementary strand, 5′-TGGTAGAC**C**TGGACGG containing a site-specific thiol-tether (indicated by **C**), and the duplex was DXLed to hOGG1 containing an engineered Cys at position-149.[4] Following purification and concentration, the DXLed complex containing O^6-photocaged oxoG (designated photocaged complex or PCC) was crystallized by the hanging droplet vapor diffusion method. A base-excision assay performed on these crystals unambiguously revealed the presence of an intact O^6-photocaged oxoG, with no evidence of processing by hOGG1 (see Supporting Information).

The structure of the PCC is similar overall to that of the G-interrogation complex,[4a] having an extrahelical target nucleobase

10.1021/ja800821t CCC: $40.75 © 2008 American Chemical Society

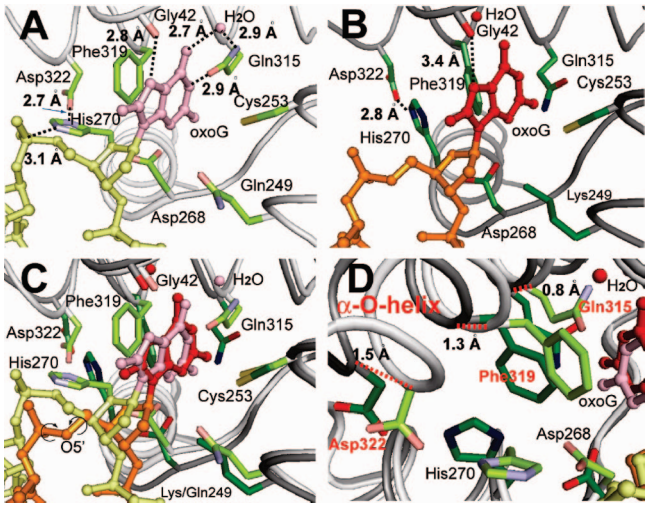

Figure 2. (A) Active site view of the hOgg1/oxoG lesion-recognition complex (LRC), with the protein backbone in light gray, side chains in green, oxoG in pink, and DNA in pale yellow. An ordered water is shown as a pink sphere. Noteworthy hydrogen bonding interactions are indicated by a dashed line. (B) Active site view of the FC (this work), with the protein backbone in dark gray; side chains, dark green; oxoG, red; DNA, gold; water, red sphere. (C) Heavy atom superposition of the FC with the LRC (color scheme as in B and A, respectively). Curved arrows denote bonds that have undergone substantial rotations. (D) Superposition as in C, but from a perspective that emphasizes the different positions of the α-O helix. Dotted line and distances illustrate the positional shifts at the C_α carbons at the residues indicated in red.

not bound in the active site, except that in the PCC the density for the caged oxoG is weak, suggesting the caged oxoG is conformationally mobile in the exosite (Supporting Information). To obtain the structure of this complex following photodeprotection (designated flashed complex or FC), crystals of the PCC were irradiated with 373 nm laser light for 30 s at 4 °C and immediately cryotrapped by being plunged into liquid nitrogen. The structure of the FC, solved to 2.8 Å resolution, reveals clear electron density for the oxoG nucleobase, but none corresponding to the photocaging group, consistent with the results of base-excision assays showing that 30 s irradiation caused >90% removal of the photocaging group (see Supporting Information). Remarkably, the oxoG lesion in the FC is inserted into the active site pocket in roughly the same position as in the hOgg1/oxoG lesion-recognition complex (LRC), which is believed to represent a state poised for catalysis (compare Figure 2 panels A and B, overlays in C and D). Indeed, the hallmark specificity-determining contact of oxoG recognition—the hydrogen bonding contact between N7−H of oxoG and the main-chain carbonyl oxygen of Gly42—is evidently present in the FC, though it is significantly longer than that observed in the LRC (3.4 vs 2.8 Å, respectively). Apart from this one signature contact, however, none of the other active site contacts to the oxoG always observed in LRC structures is formed in the FC. Three key residues known structurally and biochemically[7] to play an important role in contacting oxoG, namely Phe319, Cys253, Gln315, are all dislodged in the FC from their positions in the LRC. In addition, the contact between His270 and the oxoG 5′-phosphate is disrupted in the FC, and instead His270 stacks with Phe319. The hydrogen bonding interaction between His270 and Asp322 in the FC is not observed in the LRC, but is seen in earlier extrusion intermediates. Finally, the side chain of the catalytic nucleophile Lys249 is disordered at its distal end in the FC and does not appear to be engaged in the key salt bridge with Cys253 [Lys249(NH_3^+)/Cys253(S^-)] implicated computationally[4a] in oxoG recognition. These differences between the FC and LRC are not limited to side-chain motions. For example, the α-O helix, which bears three active site residues, Gln315, Phe319, and Asp322, is retracted from the active site in the FC (Figure 2D).

The DNA conformation in the FC is also perturbed relative to the LRC. On the 5′-side of the oxoG lesion, the DNA backbone in that region would require a crankshaft conformational shift about the oxoG $C^{4'}$-$C^{5'}$-$O^{5'}$-$P^{5'}$ to move into position for a productive contact with His270 (denoted by curved arrow in Figure 2C). The ribose ring of oxoG is shifted slightly in position, as is the catalytically essential residue Asp268.

The simplest explanation for the structural features of the FC is that it represents a very advanced intermediate in the lesion-extrusion pathway, indeed the most advanced thus far observed for any DNA glycosylase, with the oxoG nucleobase having undergone nearly complete insertion into the active site, but the protein and to some extent the DNA having not yet adopted their final, catalytically productive conformations.[8] These observations thus suggest that the transit of the lesion from the exosite to the active site occurs faster than the subsequent round of protein conformational adjustments required to produce a catalytically competent active site.

Acknowledgment. This work was supported by the NIH (CA 100742). X-ray data were collected at the 19-ID beamline at the Structural Biology Center of the Advanced Photon Source of Argonne National Laboratory. We are grateful to Brian Bowman for helpful advice with crystallography and Paul Blainey for assistance with the laser apparatus construction.

Supporting Information Available: Difference electron density map, photodeprotection assay, synthetic procedures. This material is available free of charge via the Internet at http://pubs.acs.org.

References

(1) (a) Friedberg, E. C. *Nature* **2003**, *421*, 436. (b) Krokan, H. E.; Nilsen, H.; Skorpen, F.; Otterlei, M.; Slupphaug, G. *FEBS Lett.* **2000**, *476*, 73. (c) Fromme, J. C.; Banerjee, A.; Verdine, G. L. *Curr. Opin. Struct. Biol.* **2004**, *14*, 43.
(2) (a) Lindahl, T.; Wood, R. D. *Science* **1999**, *286*, 1897. (b) David, S. S.; Williams, S. D. *Chem. Rev.* **1998**, *98*, 1221. (c) Barnes, D. E.; Lindahl, T. *Annu. Rev. Genet.* **2004**, *38*, 445.
(3) (a) Hitomi, K.; Iwai, S.; Tainer, J. A. *DNA Repair* **2007**, *6*, 410. (b) Parikh, S. S.; Putnam, C. D.; Tainer, J. A. *Mutat. Res.* **2000**, *460*, 183. (c) Stivers, J. T. *Prog. Nucleic Acid Res. Mol. Biol.* **2004**, *77*, 37.
(4) (a) Banerjee, A.; Yang, W.; Karplus, M.; Verdine, G. L. *Nature* **2005**, *434*, 612. (b) Banerjee, A.; Verdine, G. L. *Proc. Natl. Acad. Sci. U.S.A.* **2006**, *103*, 15020.
(5) (a) Burrows, C. M.; Muller, J. *Chem. Rev.* **1998**, *98*, 1109. (b) David, S. S.; O'Shea, V. L.; Kundu, S. *Nature* **2007**, *447*, 941.
(6) (a) Fromme, J. C.; Banerjee, A.; Huang, S. J.; Verdine, G. L. *Nature* **2004**, *427*, 652. (b) Huang, H.; Chopra, R.; Verdine, G. L.; Harrison, S. C. *Science* **1998**, *282*, 1669. (c) Stanojevic, D.; Verdine, G. L. *Nat. Struct. Biol.* **1995**, *2*, 450. (d) Verdine, G. L.; Norman, D. P. G. *Annu. Rev. Biochem.* **2003**, *72*, 337.
(7) (a) Radom, C. T.; Banerjee, A.; Verdine, G. L. *J. Biol. Chem.* **2007**, *282*, 9182. (b) Bruner, S. D.; Norman, D. P.; Verdine, G. L. *Nature* **2000**, *403*, 859. (c) Raducella, J. P.; Dherin, C.; Desmaze, C.; Fox, M. S.; Boiteux, S. *Proc. Natl. Acad. Sci. U.S.A.* **1997**, *94*, 8010.
(8) Kuznetsov, N. A.; Koval, V. V.; Nevinsky, G. A.; Douglas, K. T.; Zharkov, D. O.; Fedorova, O. S. *J. Biol. Chem.* **2007**, *282*, 1029.

JA800821T